Celestial Mechanics and Dynamical Astronomy (2018) 130:82
https://doi.org/10.1007/s10569-018-9875-z

ORIGINAL ARTICLE

Stability and bifurcations of even periodic orbits in the Sitnikov problem

Jorge Galán-Vioque[1] · Daniel Nuñez[2] · Andrés Rivera[2] · Camila Riccio[2]

Received: 21 January 2018 / Revised: 29 October 2018 / Accepted: 19 November 2018 /
Published online: 19 December 2018
© Springer Nature B.V. 2018

Abstract
We study different families of even periodic solutions in the classical Sitnikov problem that emanate from the circular case as the eccentricity is increased. The families can be classified by the number N of full revolutions of the primaries and labelled by the number of zeroes p of the vertical coordinate of the massless body in half a period. We give a linear stability criterion of these branches depending on even N, based on the sign for the initial slope of the discriminant function for the associated Hill's equation, in a computable interval of eccentricities. All families for $N = 2$ are linearly stable for small and computable e. The results show a fundamental symmetry-driven difference between the even and odd N cases.

Keywords Periodic orbits · Sitnikov problem · Numerical continuation

Mathematics Subject Classification 70F15 · 34B15 · 37G15 · 37N05

1 Introduction

The Sitnikov problem (Sitnikov 1960) is a special case of the restricted three-body problem where the primaries move in elliptic orbits of the two-body problem with eccentricity

This article is part of the topical collection on Recent advances in the study of the dynamics of N-body problem.
Guest Editors: Giovanni Federico Gronchi, Ugo Locatelli, Giuseppe Pucacco and Alessandra Celletti.

✉ Jorge Galán-Vioque
jgv@us.es

Daniel Nuñez
dnunez@javerianacali.edu.co

Andrés Rivera
amrivera@javerianacali.edu.co

Camila Riccio
criccio35@gmail.com

1 Applied Mathematics, Escuela Técnica Superior de Ingeniería, Universidad de Sevilla, Seville, Spain

2 Pontificia Universidad Javeriana-Cali, Cali, Colombia

$e \in [0, 1]$ and the massless body moves on a straight line perpendicular to the plane of motion of the primaries through their barycentre. In appropriate units, the equation of motion for the massless body is ruled by the differential equation

$$\ddot{z} = -\frac{z}{(z^2 + r(t, e)^2)^{3/2}}, \tag{1}$$

where $r(t, e)$ is the distance of the primaries to their centre of mass and it is given by

$$r(t, e) = \frac{1}{2}(1 - e\cos(u(t))), \tag{2}$$

and $u(t)$ is the eccentric anomaly which is a function of time through Kepler's equation

$$u - e\sin u = t\,. \tag{3}$$

In Pavanini (1907) expressed the solution by means of Weierstrass elliptic functions. A few years later, MacMillian (1913) expressed the solutions in terms of Jacobi elliptic functions. The list of analytical and numerical works on the Sitnikov problem is long (Libre and Simó 1980; Belbruno et al. 1994; Corbera and Llibre 2000, 2002; Llibre and Ortega 2008; Rivera et al. 2012; Ortega and Rivera 2010; Perdios and Markellos 1988; Robinson 2008; Dvorak 1993; Martínez-Alfaro and Chiralt 1993; Tkhai 2006; Sidorenko 2011; Soulis et al. 2007).

It is well known (Soulis et al. 2007; Sidorenko 2011) that for the circular case ($e = 0$) and a given $N \in \mathbb{N}$ there exist a finite number of nontrivial symmetric $2N\pi$-periodic solutions. All of them are parabolic and unstable (in the Lyapunov sense) if we consider the corresponding autonomous equation as a $2N\pi$-periodic equation. The authors in Llibre and Ortega (2008) proved that these families of periodic solutions can be continued from the known $2N\pi$-periodic solutions in the circular case for non-necessarily small values of the eccentricity e and in some cases for all values of $e \in [0, 1]$.

Closely related to the present paper is the numerical study of Jiménez-Lara and Escalona-Buendía (2001) where they describe numerically some families of symmetric periodic orbits for almost all values of eccentricity. However, these works do generally not provide information about the stability properties of these periodic solutions. Besides they skipped the case $N = 3$ from their analysis.

Some of the authors of the present paper provided a quantification procedure of the symmetric branches (Galán et al. 2018). They introduced new general results and applied them to the Sitnikov problem, studying the linear stability of the branches when N is odd. The present work improves on the linear stability properties of these symmetric branches when N is even, founding new and not expected properties and differences for the cases of odd or even revolutions of the primaries. We highlight the case $N = 2$ characterizing the stability properties of all branches of periodic solutions in a computable e-interval.

The paper is organized as follows: Sect. 2 is devoted to state and prove the main analytical result of this work. In Sect. 3, we describe the numerical approach to the computation of the branches. The results are classified in Sect. 2 by the number of revolutions of the primaries. The Floquet multipliers and the discriminant function are linear stability indicators that reveal the rich bifurcation structure. Here, we point out some consequences for $N = 2$ combining Theorem 2 and the results in Galán et al. (2018). In particular, we show that all families of continuation form the circular case and are elliptic for a computable e-interval. By completeness and to highlight the fundamental symmetry-driven difference between the even and odd N cases, we study numerically the cases $N = 1$ and $N = 3$. A special treatment of the case of negative eccentricity in Sect. 3.2 provides a tool to prove the vanishing of the slope of the discriminant when N is odd. We end with some conclusions and open problems

and complete the paper with some appendixes with numerical and perturbative results that complete the work.

2 Theoretical results

We present one of the main results (Theorem 1) obtained and proved in Galán et al. (2018) that will be necessary for the main results of this document. For each integer $N \geq 1$ let $\nu_N = [2\sqrt{2}N]$, where [ ] denotes the integer part function. For a fixed and p from 1 to ν_N, Theorem 1 proves the existence of a quantifying family $Z^N_{e,p}(t)$ of even and $2N\pi$-periodic solutions of the following boundary value problem

$$\ddot{z} + \frac{z}{(z^2 + r(t,e)^2)^{3/2}} = 0, \quad \dot{z}(0) = \dot{z}(N\pi) = 0, \tag{4}$$

with p zeros on $[0, N\pi]$ for all $e \in [0, e^*]$ with e^* computable. These bifurcating families emerge from even $2N\pi$-periodic solutions $\varphi_p(t) = Z^N_{0,p}(t)$ of the circular Sitnikov problem, i.e. when the eccentricity parameter e is zero.

Theorem 1 *Given an integer $N \geq 1$ and $p = 1, \ldots, \nu_N = [2\sqrt{2}N]$ there exists $\gamma = \gamma_{N,p} > 0$, $e^*_{N,p} \in [0, 1]$ explicitly computable and a smooth function $\xi = \mathcal{H}_{N,p}(e)$, $e \in [0, e^*_{N,p}]$ with $\mathcal{H}_{N,p}(0) = \xi_p$, $\varphi_p(0) = \xi_p$ such that $Z^N_{e,p}(t) = z(t; \mathcal{H}_{N,p}(e), e)$, is an even $2N\pi$-periodic solution of (4). Moreover,*

$$|Z^N_{e,p}| \leq \xi_p + \gamma e \quad for\ all \quad e \in [0, e^*_{N,p}].$$

In order to study the linear stability properties of the families $Z_e(t) := Z^N_{e,p}(t)$ in Galán et al. (2018), it is considered the *discriminant function* associated with the first variational equation along the periodic solution $Z^N_{e,p}$,

$$\ddot{y} + q(t, e, p, N)y = 0, \tag{5}$$

where $q(t, e, p, N)$ is a $2N\pi$-periodic function in t given by

$$q(t, e, p, N) := \frac{r(t,e)^2 - 2Z^N_{e,p}(t)^2}{(Z^N_{e,p}(t)^2 + r(t,e)^2)^{5/2}}. \tag{6}$$

The *discriminant function* associated to the Hill's equation (5) is defined by

$$\Delta(e) = y_1(2N\pi, e) + \dot{y}_2(2N\pi, e), \tag{7}$$

where $y_i(t, e)$, $i = 1, 2$ are the canonical solutions of (5), satisfying

$$y_1(0, e) = \dot{y}_2(0, e) = 1, \qquad \dot{y}_1(0, e) = y_2(0, e) = 0.$$

Notice that $\Delta(e)$ is the trace of the monodromy matrix $\Phi(e)$ associated to the first order planar system associated to (5). On the other hand, it is well known (see Magnus and Winkler 1979; Jury 1975) that (5) is stable (equivalently Z_e is *linearly stable*) if and only if the corresponding Floquet multipliers $\rho_i[e]$, $i = 1, 2$ satisfy one of the following conditions:

(A1) $\rho_1 = \overline{\rho_2} \notin \mathbb{R}$, $|\rho_{1,2}| = 1$, equivalent to $|\Delta(e)| < 2$.
(A2) $\rho_{1,2} = \pm 1$ (equivalent to $|\Delta(e)| = 2$) and $\Phi(e) = \pm I_d$ being I_d the 2×2 identity matrix,

and is *unstable* (equivalently Z_e is *linearly unstable*) if

(A3) $\rho_{1,2} = \pm 1$ (equivalent to $|\Delta(e)| = 2$) and $\Phi(e) \neq \pm I_d$.
(A4) $|\rho_1| < 1 < |\rho_2|$, $\rho_i \in \mathbb{R}$, $i = 1, 2$ (equivalent to $|\Delta(e)| > 2$).

Furthermore, Eq. (5) is called

I. *Elliptic* if condition (A1) holds.
II. *Parabolic Stable (Unstable)* if condition (A2)((A3)) holds.
III. *Hyperbolic* if condition (A4) holds.

For the case $e = 0$ (the circular case), it follows that $\Delta(0) = 2$ since the function $\dot{\varphi}_p$ is an odd and $2N\pi$-periodic solution of (5) (as a direct computation shows) and therefore $\rho_{1,2}(0) = 1$. Furthermore, it can be proven that $\Phi(0) \neq I_d$ therefore Z_0 is *linearly unstable* (see Magnus and Winkler 1979). From here, we deduce that the linear stability properties of Z_e for e small will depend on the properties of the functions $\Delta'(e)$, $\Delta''(e)$...
In Galán et al. (2018), we derived the analytic formulas for $\Delta'(e)$ and $\Delta''(e)$, which are given by

$$\begin{aligned} \Delta'(e) &= \int_0^{2N\pi} w(s,e)\partial_e q(s,e)\mathrm{d}s, \\ \Delta''(e) &= \int_0^{2N\pi} \Big(\partial_e w(s,e)\partial_e q(s,e) + w(s,e)\partial_e^2 q(s,e)\Big)\mathrm{d}s, \end{aligned} \tag{8}$$

where $w(s,e) = \dot{y}_1(2N\pi, e)y_2^2(s,e)$. The sign of $\Delta'(0)$ clearly implies the stability result for the linearized equation (5) for small e. Keeping this in mind, we need the following result.

Lemma 1 *Let $h \in C^2([0,E])$ with $h(0) = 0$, $h'(0) = m$. Let $K > 0$ be an upper bound for $|h''(x)|$ for all $x \in [0,E]$, i.e.*

$$\max_{x\in[0,E]} |h''(x)| \leq K.$$

We have,

(1) *If $m > 0$ then $h(x) > 0$ for all $x \in]0, E_1]$ where $E_1 = \min\left\{E, \dfrac{2m}{K}\right\}$*
(2) *Let $\alpha > 0$ fixed. If $m < 0$ then $-\alpha < h(x) < 0$ for all $x \in]0, E_2]$ where*

$$E_2 = \min\left\{E, -\frac{2m}{K}, \frac{m + \sqrt{m^2 + 2\alpha K}}{K}\right\}.$$

Proof Consider the Taylor's expansion of $h(x)$ at $x = 0$ given by

$$h(x) = mx + R(x),$$

where the remainder $R(x)$ satisfies

$$|R(x)| \leq \max_{x\in[0,E]} |h''(x)|\frac{x^2}{2} \leq \frac{Kx^2}{2}.$$

In consequence,

$$\big(m - (Kx)/2\big)x \leq h(x) \leq \big(m + (Kx)/2\big)x, \tag{9}$$

for all $x \in [0, E]$. In the case of positive slope ((1)$m > 0$) it follows

$$0 < m - (Kx)/2 \Leftrightarrow x < \frac{2m}{K}.$$

Combining this last inequality with (9), we deduce that $h(x) > 0$ for all $x \in [0, E_1]$ where $E_1 = \min\left\{E, \dfrac{2m}{K}\right\}$.
In the case of negative slope ((2) $m<0$), for any give α we deduce from (9) that the inequalities $-\alpha < h(x) < 0$ hold if

$$-\alpha < \big(m - (Kx)/2\big)x \quad and \quad \big(m + (Kx)/2\big)x < 0.$$

For $x \geq 0$, these last two inequalities are equivalent to

$$x < \frac{m + \sqrt{m^2 + 2\alpha K}}{K}, \quad \text{and} \quad x < -\frac{2m}{K}.$$

If we define $E_2 = \min\left\{E, -\dfrac{2m}{K}, \dfrac{m + \sqrt{m^2 + 2\alpha K}}{K}\right\}$ then $-\alpha < h(x) < 0$ for all $x \in [0, E_2]$. This completes the proof. □

Define

$$\upsilon = \Delta'(0), \qquad \mathcal{K}^* \geq \max_{e \in [0, e^*_{N,p}]} |\Delta''(e)|,$$

$$\mathcal{E}_1^* = \min\left\{e^*_{N,p}, \frac{2\upsilon}{\mathcal{K}^*}\right\}, \qquad \mathcal{E}_2^* = \min\left\{e^*_{N,p}, -\frac{2\upsilon}{\mathcal{K}^*}, \frac{\upsilon + \sqrt{\upsilon^2 + 8\mathcal{K}^*}}{\mathcal{K}^*}\right\}.$$

In "Appendix A", we give a computable value of $\mathcal{K}^*$ given by the formula (15).

Theorem 2 *Let $N \in \mathbb{N}$ and $p = 1$ to $\nu_N = [2\sqrt{2}N]$ fixed. Let $\Delta(e)$ the discriminant function of (5) for $e \in [0, e^*[$ where $e^* = e^*_{N,p}$ given by Theorem 1. Assume the condition $\Delta'(0) = \upsilon \neq 0$. Then,*

i) *If $\upsilon > 0$ the periodic solution $Z^N_{e,p}$ of (4) is linearly unstable $\forall e \in]0, \mathcal{E}_1^*]$.*
ii) *If $\upsilon < 0$ the periodic solution $Z^N_{e,p}$ of (4) is linearly stable $\forall e \in]0, \mathcal{E}_2^*]$.*

Proof For any fixed $N \geq 1$ and $p = 1$ to ν_N fixed, we apply Lemma 1 to the function $h \in C^2([0, e^*_{N,p}])$ defined by $h(e) = \Delta(e) - 2$. Notice that

$$h(0) = \Delta(0) - 2 = 0, \quad h'(0) = \Delta'(0) = \upsilon.$$

If the assumption in (i) hold, i.e. $\upsilon > 0$ then

$$0 < h(e) \Leftrightarrow \Delta(e) > 2,$$

for all $e \in [0, \mathcal{E}_1^*]$. Therefore, the Eq. (5) is *hyperbolic* which means that $Z^N_{e,p}$ is linearly unstable.
If the assumption in ii) holds, i.e. $\upsilon < 0$ then

$$-4 < h(e) < 0 \Leftrightarrow -2 < \Delta(e) < 2,$$

for all $e \in [0, \mathcal{E}_2^*]$. Therefore, Eq. (5) is *elliptic* which means that $Z^N_{e,p}$ is linearly stable. This completes the proof. □

Remark 1 When N is odd, it is possible to prove that $\upsilon = 0$ (see Galán et al. 2018), henceforth Theorem 2 does not provide information about the stability properties of $Z^N_{e,p}$. The case N odd is considered in Theorem 2 in Galán et al. (2018) taking in account the sign of $\Delta''(0)$.

On the other hand, the key value υ in Theorem 2 has been computed in a general Newtonian equation with a nonlinear centre at the origin (see Zhang et al. 2018), based on the $2N\pi$-periodic solutions $\varphi(t)$ in the circular case ($e = 0$) and on some information about their canonical solution $\phi(t) = y_1(t, 0)$:

$$\upsilon = \Delta'(0) = \frac{\phi_1'(2N\pi, 0)}{4\mu^2} \int_0^{2N\pi} \frac{\cos s}{\left(\varphi(s)^2 + \frac{1}{4}\right)^{\frac{3}{2}}} \mathrm{d}s, \tag{10}$$

where

$$\mu = f(\xi_p, 1/2), \quad f(z, r) = \frac{z}{(z^2 + r^2)^{3/2}}.$$

3 Numerical results

The search of periodic orbits that emanate from the circular case ($e = 0$) can be easily formulated as a standard continuation procedure on the BVP problem (4). But this problem provides only half of the orbit; to reconstruct the full orbit, we make use of the symmetry and extend to the full period of the orbit which is $T = 2N\pi$. The boundary conditions ensure that all the solutions of (4) extended to the time interval $[0, T]$ are periodic and even in t.

We have made use of the continuation procedure presented in Muñoz-Almaraz et al. (2003) for the conservative case and later extended to properly treat the symmetries and reversibilities in Muñoz-Almaraz et al. (2007). See also Galán-Vioque et al. (2014) for a review and examples from Mechanics.

In the Sitnikov problem, a two-step procedure has been necessary; first we have continued the circular family of period orbits for $e = 0$ (Hamiltonian case) that can be parametrized by the period which turns out to be a monotonically increasing function. Along these family of periodic solutions for $e = 0$ (circular case) we have detected the initial conditions $\xi(0)$ whose associated period is commensurate with that of the primaries. Precisely with that initial condition, we have computed by the initial value integration an appropriate starting solution for the emanating branch that was the input to a boundary value continuation in the eccentricity.

The continuation algorithm is implemented in AUTO which is a well tested and accurate program for numerical continuation based on collocation and a pseudo arclength strategy (Doedel et al. 1997). In "Appendix B", we cast all the initial vertical separation of the massless body for the 15 branches considered in this paper.

The initial value of the period of the oscillatory motion of the primary can be obtained by the Lyapunov Center Theorem and is given by $T_c = \frac{2\pi}{2\sqrt{2}}$. Since the Kepler problem in the appropriate units is 2π, the resonance condition is thus $N2\pi = p2\sqrt{2}$ where p is the number or periods of the primary. As stated in Llibre and Ortega (2008), the maximum value of p for a given value of N is ν_N. In this paper, we will thoroughly investigate the cases $N = 1, 2$ and 3 which correspond to $\nu_1 = 2$, $\nu_2 = 5$ and $\nu_3 = 8$. Therefore, we will follow at most 15 branches of periodic orbits.

The conclusion of this argument is that the branches can be labelled by N and p where p is the number of zeros of the z component of the massless body in half a period $[0, N\pi]$. As a by-product of the numerical continuation, we compute with negligible cost the multipliers of the $2N\pi$-periodic solution and detect the possible bifurcations and the discriminant function $\Delta(e)$ defined in the previous section as the trace of the monodromy matrix.

The final outcome of the calculation is a branch in the ξ, e plane for each N and p and the linear stability of the associated periodic solutions.

For $N = 1$, 2 and 3, we plot the Floquet multipliers and the discriminant function $\Delta(e)$ for all values of p and $0 \leq e < 1$ for the branches that emanate from the circular case ($e = 0$). All the branches for fixed value of N are plotted in a bifurcation ξ,e diagram indicating the linear stability with a solid blue line and the instability with a dashed red line.

3.1 Case $N = 1$

For $N = 1$, the primaries perform just a single complete revolution before the massless body returns to its initial condition. There are only two branches corresponding to even periodic orbits. Both are born linearly stable from the circular problem and the initial linear stability remains up to moderate values of e ($e \sim 0.5$ and 0.9, respectively). The Floquet multipliers start from $+1$ (parabolic case) and rotate on the unit circle until the -1 is reached where they split in a *period doubling bifurcation* (PD). The branches remain unstable up to $e = 1$ where a collision between the primaries takes place. At the PD bifurcation, a new elliptic family with double period is born. This secondary branch has been computed but is not displayed for the sake of clarity. In general, it follows a period doubling cascade leading to chaotic behaviour. These two primary branches were considered as numerical examples for the quantitative study of the elliptic branches in Galán et al. (2018). Note that for both branches, $\Delta'(0) = 0$ and the stability will be determined by the second derivative of the discriminant function. At the period doubling bifurcation, the logarithm of the modulus of the multipliers depart from zero in a symmetric way (if ρ is a multiplier so is $1/\rho$), and the principal argument of the multipliers reach $+\pi$ and $-\pi$, respectively. This kind of PD bifurcations is usually called *splitting PD* bifurcations because the multipliers depart from the unit circle and the original branch loses its stability (Figs. 1 and 2).

3.2 Negative eccentricity results for N odd

In Galán et al. (2018), we were able to prove that for odd values of N the discriminant function is an even function of the eccentricity [see Proposition 4.2 in Galán et al. (2018)].

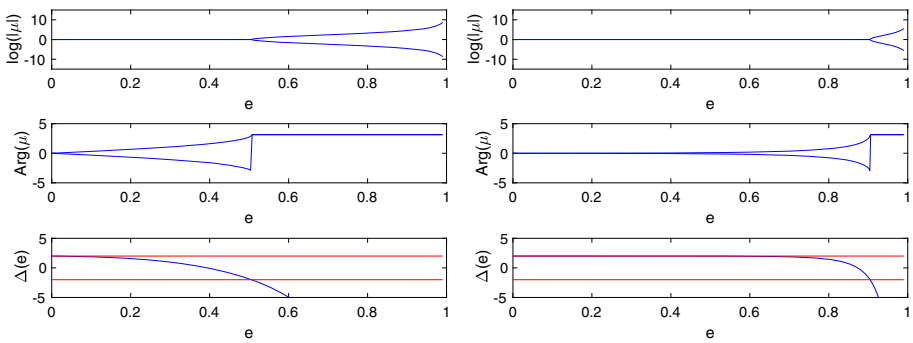

Fig. 1 Floquet multipliers for the two branches corresponding to $N = 1$. The left subplot corresponds to $p = 1$ and the right one is $p = 2$. In this and the following figures representing Floquet multipliers, the upper panel is the logarithm of the modulus of the multipliers whereas the middle panel shows its principal argument as a complex number. The lower panel shows the discriminant function $\Delta(e)$ (in blue). The two red horizontal lines border the stable region indicating branching point bifurcation ($+2$) and period doubling (-2)

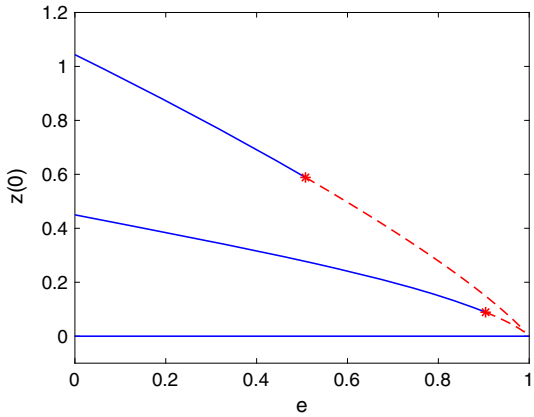

Fig. 2 Bifurcation diagram for the two branches corresponding to $N = 1$. The upper curve corresponds to $p = 1$ (one zero of $z(t)$ in half a period) whereas the lower one corresponds to $p = 2$ (two zeros in half a period). Both branches behave in a similar way and are born as linearly *elliptic* and remain so up to intermediate ($p = 1$) and high ($p = 2$) values of e. The red asterisks denote the splitting PD bifurcations

From the modelling point of view, it is unclear the meaning and usefulness of $e < 0$ but from the mathematical point of view it is a valid extension. This evenness immediately proves the vanishing of the slope of the discriminant of the $\Delta(e)$ function at the origin.

The authors of Zhang et al. (2018) have also proven independently and with a different technique the vanishing of $\Delta'(0)$ only for the case $N = 1$. In fact, they provide an elegant expression (see Eq. 10) for its value that will be used in "Appendix C".

In the next subsection and in "Appendix B", we will show that for even values of N, the quantity $\Delta'(0)$ does not have to be zero necessarily. In our opinion, this is an interesting and nontrivial result; there are *qualitative differences* between the odd and even N cases.

3.3 Case $N = 2$

For $N = 2$, we have 5 branches emanating from the circular case. It is easy to see that the $N = 2$ and $p = 2$ circular solutions are equivalent to twice the $N = 1$ and $p = 1$ one. The same holds for $N = 2$ $p = 4$ and $N = 1$ $p = 2$. These branches for different values of N coincide in the ξ, e plane but the multipliers are shifted in e corresponding to the second iterate of the Poincaré map. For example, a PD bifurcation (multiplier at -1) for $N = 1$ $p = 1$ corresponds to a branching point (BP) (multiplier at $+1$) for the $N = 2$ $p = 2$.

The multipliers corresponding to $p = 1, 2, 3$ and 4 are displayed in Fig. 3 and exhibit an interesting bifurcation behaviour.

The most remarkable case is $p = 1$ which turns out to be the only symmetric branch for which $\Delta'(0) \neq 0$. In this case, with negative slope which means that the stability of the solutions changes from unstable into stable as the eccentricity crosses from negative to positive values. The branch is initially stable and undergoes a "passing" period doubling ($e \sim 0.15$) without loss of stability (the multipliers cross at $+1$ without leaving the unit circle). The discriminant function undergoes a tangency at $\Delta(e^*) = -2$. We find also a window of instability for $p = 1$ at a BP bifurcation at $e \sim 0.55$. The stability is regained later at $e \sim 0.85$ and the branch remains stable up to the collision at $e \sim 1$.

Branches $p = 2$ and $p = 3$ behave similarly with a passing PD and a loss of stability at a BP. Both branches start with zero slope for the discriminant function. Branch $p = 4$ is stable up to a PD bifurcation at $e \sim 0.88$.

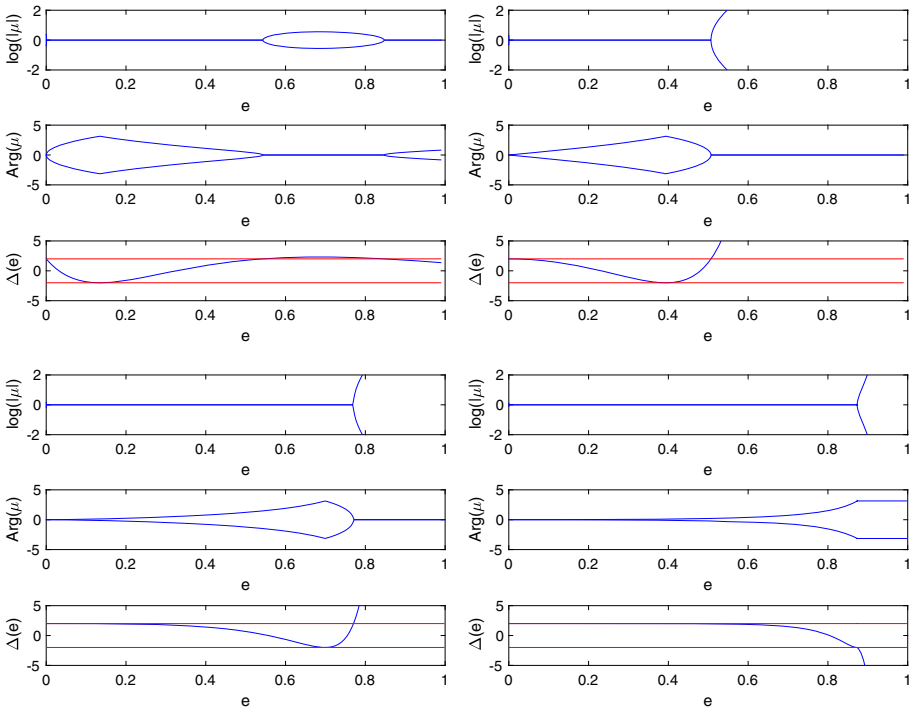

Fig. 3 In these four sub-panels, we plot the behaviour of the Floquet multipliers for the branches corresponding to $N = 2$ and $p = 1, 2, 3$ and 4 in clockwise order with the same procedure as previous cases. The general behaviour is *qualitatively* different form the odd-N cases (see $N = 1$ above and $N = 3$ later)

The branch with smaller value of $\xi(0)$ that corresponds to $p = 5$ is analysed in detail in Fig. 4. A careful monitoring of the stability indicators reveals another window of instability along the branch.

In Fig. 5, we extend the range of e to negative values and zoom around $e = 0$. Note that in this case $\Delta'(0) \neq 0$. We have checked the correctness of this result by evaluating analytically the slope of the $\Delta(e)$ curve with the expressions presented in "Appendix C". The case of N even is fundamentally different from N odd. However, for the 4 remaining branches corresponding to $N = 2$ even the discriminant starts with zero slope.

To end this subsection, we plot the partial bifurcation diagram for $N = 2$ with the same notation used for $N = 1$.

3.4 Case $N = 3$

When the primaries are allowed to perform three complete revolutions before the periodic orbit is closed ($N = 3$), we know that there exist eight even in time periodic solutions of the negligible mass along the vertical axis. They are again labelled by the number of zeros (i.e. crossings of the horizontal plane) in half a period from $p = 1$ up to $p = 8$. As in the previous section, it is easy to prove that the cases $N = 3$, $p = 3$ is the same branch as $N = 1$, $p = 1$ and with $N = 3$ $p = 6$ and $N = 1$, $p = 2$ but with three identical full sequential revolutions. Again, the corresponding bifurcation of the multipliers can be deduced from the $N = 1$ case by a rigid rotation of the multipliers around the unit circle (Fig. 6).

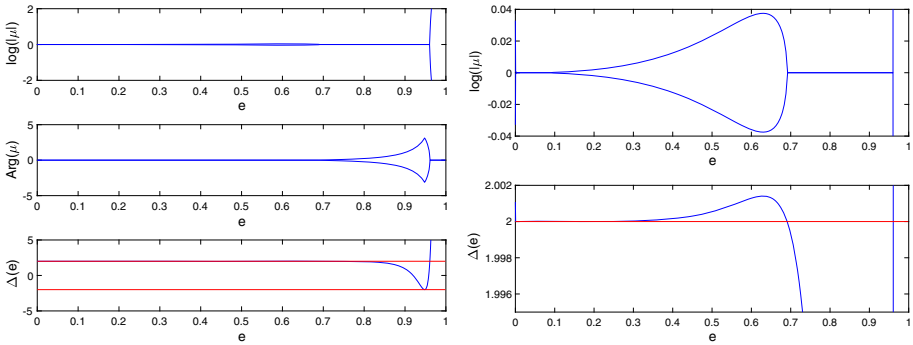

Fig. 4 In this figure in the left sub-panel, we present the Floquet multipliers for $N = 2$ and $p = 5$. At a first glance, the branch seems to be stable up to $e \sim 0.95$ where a splitting BP occurs just after a passing PD similar to the other branches. However, a closer look at the stability indicators [principal argument of the multipliers (above) and discriminant function (below)] in the right sub-panel shows that the branch undergoes a instability window with two BP bifurcations approximately at $e \sim 0.1$ and $e \sim 0.7$ where the elliptic behaviour is recovered

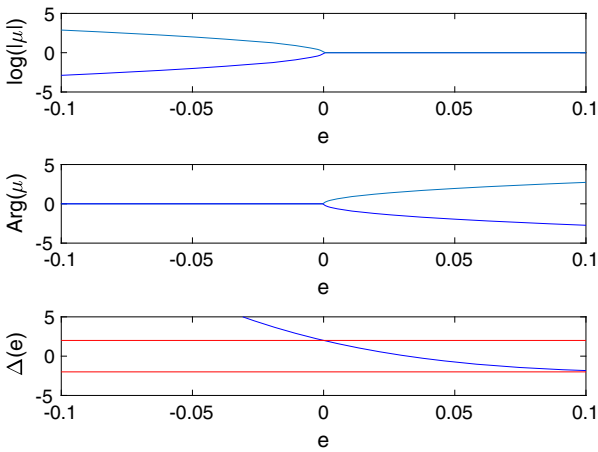

Fig. 5 Floquet multipliers and discriminant function as a function of the eccentricity for positive and negative values for branch $N = 2$ and $p = 1$

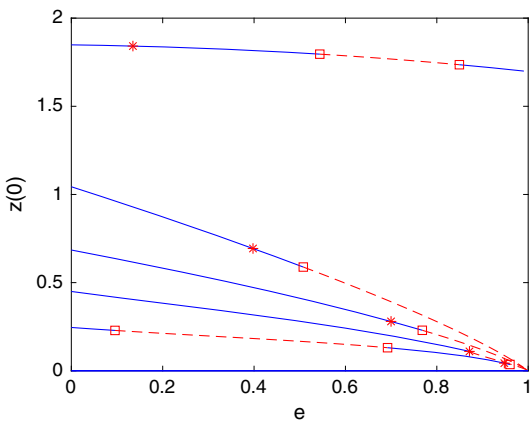

Fig. 6 Bifurcation diagram for the 5 branches corresponding to $N = 2$. The upper curve corresponds to $p = 1$ (only one zero of $z(t)$ in half a period) and as discussed above presents a non-standard behaviour for the discriminant function ($\Delta'(0) \neq 0$). The following four branches downwards correspond to $p = 2, 3, \ldots 5$ (with p zeros in half a period). We have indicated the passing PD and BP bifurcations as explained in the corresponding figures of the Floquet multipliers, i.e. Figs. 3 and 4

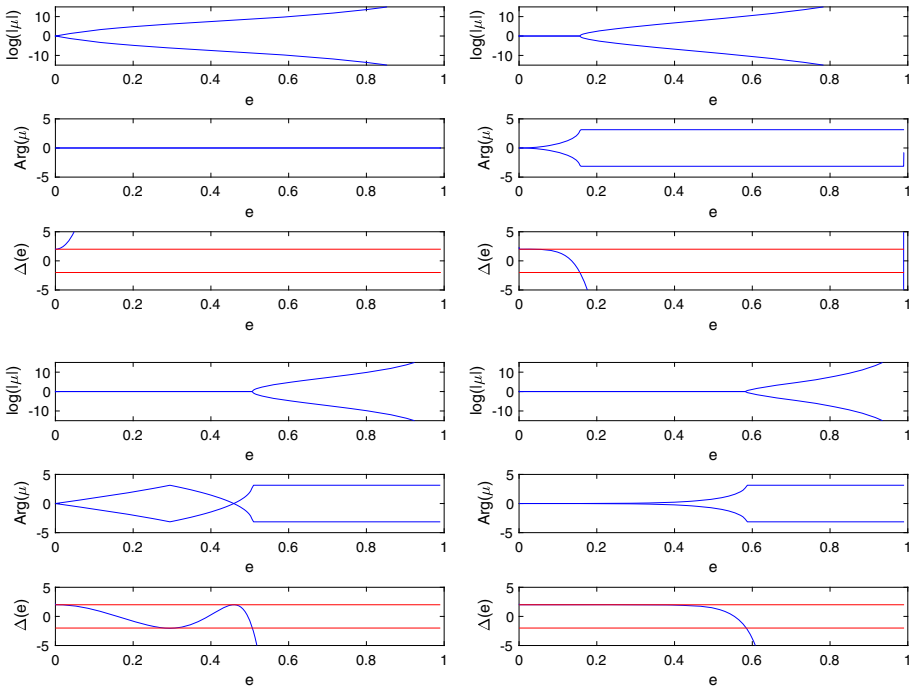

Fig. 7 In these four sub-panels, we plot the behaviour of the Floquet multipliers for the branches corresponding to $N = 3$ and $p = 1, 2, 3$ and 4 in clockwise order with the same procedure as previous cases. The most remarkable case is $p = 1$ which turns out to be the only symmetric branch which starts as hyperbolic (unstable) right from $e = 0$ but with $\Delta'(0) = 0$. The branch corresponding to $p = 3$ undergoes a PD and BP bifurcation of the passing type (not leaving the unit circle and with a tangency of the discriminant function to the threshold lines) before the splitting PD at $e \sim 0.4$. As explained in the text, this branch is equivalent to $N = 1$, $p = 1$ but with 3 full revolutions of the orbit and the passing bifurcations are the signatures of the subharmonic bifurcations corresponding to a multipliers equal to the square and third root of unity in the $N = 1$ and $p = 1$ branch

In Figs. 7 and 8, we plot in four sub-panels the Floquet multipliers with the same procedure of the previous cases, i.e. log of the modulus, principal argument and discriminant function.

We should point out that in all 8 cases numerically it holds that $\Delta'(0) = 0$, in agreement with Proposition 4.2 in Galán et al. (2018) of the even in e character of the function $\Delta(e)$.

Branches 2 through 8 behave in a similar way to the case $N = 1$, i.e. they start as linearly *elliptic* and loses their stability via a period doubling bifurcation before reaching the vicinity of $e = 1$ region. In some cases (precisely for the above-mentioned $p = 3$ and 6 cases), before reaching the stability losing period doubling they cross on the unit circle trough a Branching Point (BP) and a period doubling (PD) bifurcation in which there is no change of stability (passing BP or PD where the multipliers meet and remain at the unit circle). Those are the well-known subharmonics bifurcations.

Branch corresponding to $p = 1$ is *qualitatively* different form the rest; it is hyperbolic (unstable) right from the beginning. The Floquet multipliers split along the real axis (one inside and one outside, as they should) and remain real along the branch; correspondingly the discriminant function raises from the border at $+2$ with zero slope. However, the condition $\Delta'(0) = 0$ is still valid and the stability is determined by the its second derivative. We would like to highlight that this is the only hyperbolic symmetric solution that we have found for the 15 branches under consideration in this paper.

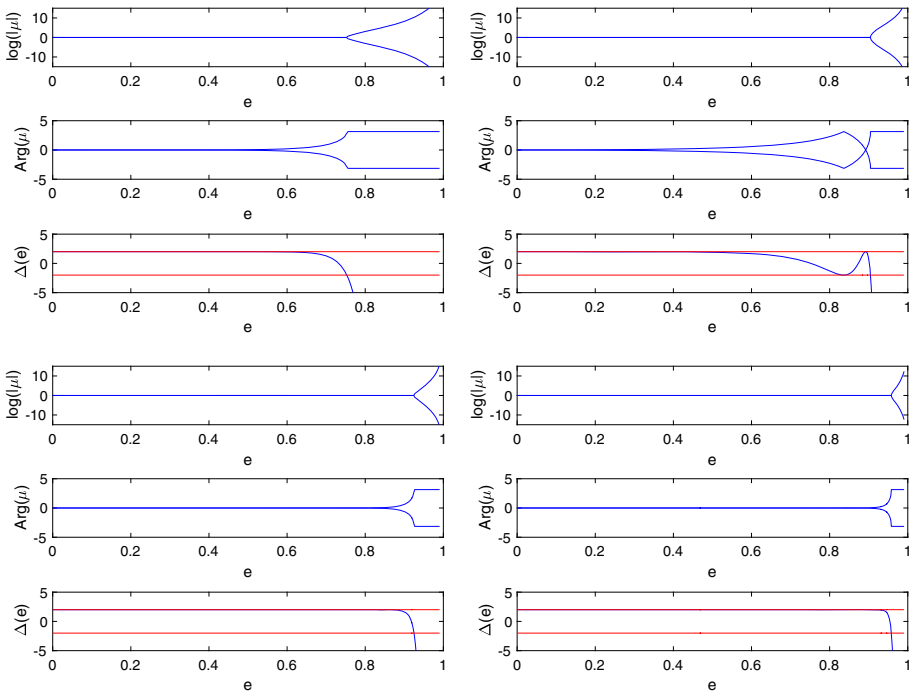

Fig. 8 These four sub-panels show the remaining four branches for $N = 3$ corresponding to $p = 5, 6, 7$ and 8. All of them start as linearly elliptic and $p = 6$ corresponds to the third iterate of $N = 1$ and $p = 2$ exhibiting the corresponding passing PD and BP before the splitting PD bifurcation close to $p = 0.9$

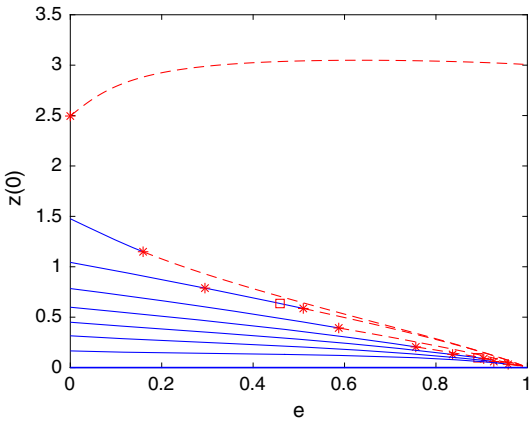

Fig. 9 Bifurcation diagram for the 8 branches corresponding to $N = 3$. The upper curve corresponds to $p = 1$ (only one zero of $z(t)$ in half a period) and as discussed above is hyperbolic (red dashed curve) just form its start at the circular problem. Note that this is the only solution which turns up with e. The following 7 branches heading downwards correspond to $p = 2, 3, \ldots 8$ (with p zeros in half a period). All these branches behave in a similar way and are born as linearly *elliptic* and remain so up to consecutively higher values of e where the stability is lost via a PD bifurcation. In branches $p = 3$ and $p = 6$, we have indicated the passing PD and BP bifurcations as that appear as explained in the corresponding figures of the Floquet multipliers, i.e. Figs. 7 and 8

All 8 branches are cast in a partial bifurcation diagram in Fig. 9. The unstable branch for $p = 1$ behaves differently form the rest and start with positive slope to higher values of the initial displacement of the zero mass body. We have checked the correctness of this result by evaluating analytically via the implicit function theorem the slope of the $\xi(e)$ curve with the expressions presented in "Appendix C".

We could merge all three bifurcation diagram but without an appropriate nonlinear rescaling it would be difficult to observe the bifurcation structure.

4 Conclusions

The linear stability criterion for the even $2\pi N$-periodic continuation families from the circular case for N even is based on a first approximation on the sign of a slope. This sign can be computed using information of the starting $2\pi N$-periodic circular solutions. We have performed a detailed numerical analysis of all the symmetric branches in the elliptic Sitnikov problem when the primaries are allowed to perform 1, 2 or 3 full revolutions.

The main conclusion is the fact that the cases with odd N are qualitatively different from the even N cases. In the first cases, the discriminant function vanishes for all values of p, whereas for the second cases the slope of the discriminant function may take nonzero values for some branches.

All the branches considered in this paper extend up to $e \sim 1$, which is a clear indication that from the two possibilities considered in the main theoretical result of paper (Llibre and Ortega 2008) (global continuation of reconnection to the equilibrium point solution on the plane of the primaries) the first one is the only numerically observed for symmetric solutions and $N \leq 3$.

The agreement between the theoretical predictions and the numerical results is remarkable.

It would be interesting to compute the Birkhoff coefficient along the elliptic branches to prove the nonlinear stability. The application of the techniques developed by Ortega (1992, 1996) is confident that the technical difficulties may be overcome. Results along this line will be reported elsewhere.

Acknowledgements The authors acknowledge fruitful discussions with Rafael Ortega on related topics. JGV's research has been financially supported by the Spanish Ministry of Economy through Grant MTM2015-65608-P and Junta de Andalucía Excellence Grant P12-FQM-1658. The authors D. Nuñez and A. Rivera have been financially supported by the Capital Semilla (2015–2016) project 020100480.

Appendix A: Upper bound for $|\Delta''(e)|$

For any given $N \geq 1$ and $p = 1$ to ν_N, this appendix is devoted to compute an upper bound for $|\Delta''(e)|$ where $\Delta''(e)$ is given by

$$\Delta''(e) = \int_0^{2N\pi} \big(\partial_e w(s,e)\partial_e q(s,e) + w(s,e)\partial_e^2 q(s,e)\big)\mathrm{d}s.$$

Then, it is necessary to find global bounds on $[0, e^*]$ of the functions $w(t,e)$, $\partial_e w(t,e)$ and $q(t,e) := q(t,e,p,N)$ with

$$w(t,e) = \dot{y}_1(2N\pi, e)y_2^2(t,e), \quad q(t,e) = \frac{r(t,e)^2 - 2Z_{e,p}^N(t)^2}{(Z_{e,p}^N(t)^2 + r(t,e)^2)^{5/2}},$$

where $Z_e(t) := Z^N_{e,p}(t)$ is the periodic solution of (4) and $y_i(t,e)$ $i = 1, 2$ are the canonical solutions of (5). Following the results in Galán et al. (2018) (see Sect. 3.1), we have

$$\|w\|_\infty \le \mathcal{R}^2, \quad \text{and} \quad \|\partial_e w\|_\infty \le 3\mathcal{R}^2,$$

with $\mathcal{R}$ a positive and computable constant. For future computations, we will be using that $q(t,e)$ can be written in the following way

$$q(t,e) = F(t,e)H(t,e),$$

where

$$F(t,e) = r(t,e)^2 - 2Z_e^2(t), \quad H(t,e) = \left(Z_e^2(t) + r(t,e)^2\right)^{-5/2};$$

in this way

$$\begin{aligned} \partial_e q &= F\,\partial_e H + \partial_e F\,H \\ \partial_e^2 q &= F\,\partial_e^2 H + 2\partial_e F\,\partial_e H + \partial_e^2 F\,H. \end{aligned}$$

A straightforward computation shows that

$$\begin{aligned} \partial_e F &= 2r\partial_e r - 4Z_e\,\partial_e Z_e \\ \partial_e^2 F &= 2\big((\partial_e r)^2 + r\partial_e^2 r - 2\big((\partial_e Z_e)^2 + Z_e\,\partial_e^2 Z_e\big)\big) \end{aligned} \tag{11}$$

and

$$\begin{aligned} \partial_e H &= -5\left(\frac{Z_e}{(Z_e^2+r^2)^{7/2}}\,\partial_e Z_e + \frac{r}{(Z_e^2+r^2)^{7/2}}\,\partial_e r\right) \\ \partial_e^2 H &= \frac{35\big(Z_e\,\partial_e Z_e + r\partial_e r\big)^2}{(Z_e^2+r^2)^{9/2}} - \frac{5\big((\partial_e Z_e)^2 + Z_e\,\partial_e^2 Z_e + (\partial_e r)^2 + r\,\partial_e^2 r\big)}{(Z_e^2+r^2)^{7/2}}. \end{aligned} \tag{12}$$

At this point, it is convenient to recall some upper bounds given in Galán et al. (2018) (see Sect. 3). Therefore, for all $(t,e) \in \mathbb{R} \times [0, e^*]$ we have, with $\gamma = \gamma_1$

$$\begin{aligned} |Z_e| &\le \xi_p + e\gamma_1 := \mathcal{G}(e), \quad |\partial_e Z_e| \le \gamma_1 \\ |r| &\le \frac{1+e}{2} := r_0(e) \quad \partial_e r| \le \frac{1}{2(1-e)} := r_1(e). \end{aligned}$$

In order to obtain upper bounds for $\partial_e^2 F$ given in (11) and $\partial_e^2 H$ given in (12) only remains to compute upper bounds for $\partial_e^2 r$ and $\partial_e^2 Z_e$.

Upper bound for $\partial_e^2 r$. From Eq. (2), we have

$$\partial_e^2 r = \frac{\sin^2 u}{2r} + \frac{e}{4r^2}(\cos u - \partial_e r)\sin u.$$

After some easy computations, it follows

$$|\partial_e^2 r| \le \frac{2-e}{2(1-e)^3} := r_2(e).$$

Upper bound for $\partial_e^2 Z_e$. We know that the function Z_e satisfies

$$\ddot{z} + f(t,z,e) = 0, \quad \dot{Z}_e(0) = \dot{Z}_e(N\pi) = 0,$$

where

$$f(t,z,e) = \frac{z}{(z^2 + r(t,e)^2)^{3/2}}.$$

In consequence, $\partial_e^2 Z_e(t)$ is the solution of

$$\ddot{y} + q(t,z,e)y + B(t,z,e) = 0, \quad y(0) = 0, \quad \dot{y}(0) = 0$$

with

$$B(t,z,e) = \partial_z q(t,z,e)\,\partial_e Z_e(t) + \partial_e q(t,z,e) + \partial_{ze}^2 f(t,z,e)\,\partial_e Z_e(t) + \partial_e f(t,z,e).$$

Using the method of variation of parameters, we deduce that

$$\partial_e^2 Z_e(t) = -\int_0^t G(t,s,e)\,B(s,Z_e,e)\mathrm{d}s,$$

where $G(t,s,e) = y_1(s,e)y_2(t,e) - y_1(t,e)y_2(s,e)$. In consequence,

$$|\partial_e^2 Z_e| \leq T\,\||G\|_\infty\,\|B\|_\infty\,.$$

Once again, following the results in Galán et al. (2018) (see Sect. 3.1 and "Appendix A") we found and deduce bounds for G and b, respectively. Then

$$\|G\|_\infty \leq 2\mathcal{R}^2, \quad \|B\|_\infty \leq b(e),$$

where

$$b(e) = \frac{12(1+16\gamma_1)}{(1-e)^4} + \frac{96(1+\gamma_1)(1+3N\pi\sigma\mathcal{R}^2)}{(1-e)^4}.$$

Therefore,

$$|\partial_e^2 Z_e| \leq 4N\pi\mathcal{R}^2 b(e) := \gamma_2(e).$$

In summary, the previous computations allow us to conclude the following:

$$\begin{aligned}
|F| &\leq r_0^2(e) + 2\mathcal{G}^2(e)\\
|\partial_e F| &\leq 2r_0(e)r_1(e) + 4\gamma_1\,\mathcal{G}(e)\\
|\partial_e^2 F| &\leq 2\big(r_1^2(e) + r_0(e)r_2(e) + 2\big(\gamma_1^2 + \mathcal{G}(e)\gamma_2(e)\big)\big),
\end{aligned}$$

which is equivalent to

$$\begin{aligned}
|F| &\leq \frac{(1+e)^2}{4} + 2\mathcal{G}^2(e)\\
|\partial_e F| &\leq \frac{1+e}{2(1-e)} + 4\gamma_1\,\mathcal{G}(e)\\
|\partial_e^2 F| &\leq 2\left(\frac{2-e^2}{4(1-e)^2} + 2\big(\gamma_1^2 + \mathcal{G}(e)\gamma_2(e)\big)\right)
\end{aligned} \tag{13}$$

and

$$\begin{aligned}
|H| &\leq \frac{1}{r^5}\\
|\partial_e H| &\leq \frac{2^6\,5}{(1-e)^7}\big((1+e)r_1(e) + 2\gamma_1\mathcal{G}(e)\big)\\
|\partial_e^2 H| &\leq \frac{35\big(\gamma_1\mathcal{G}(e) + r_0(e)r_1(e)\big)^2}{r^9} + \frac{5\big(\gamma_1^2 + \gamma_2(e)\mathcal{G}(e) + r_1^2(e) + r_0(e)r_2(e)\big)}{r^7},
\end{aligned}$$

which is equivalent to

$$
\begin{aligned}
|H| &\leq \frac{2^5}{(1-e)^5} \\
|\partial_e H| &\leq \frac{2^5\, 5}{(1-e)^7}\left(\frac{1+e}{(1-e)} + 4\gamma_1 \mathcal{G}(e)\right) \\
|\partial_e^2 H| &\leq \frac{2^7\, 5}{(1-e)^7}\left(\frac{28}{(1-e)^2}\left(\gamma_1\mathcal{G}(e) + \frac{1+e}{4(1-e)}\right)^2\right) + \frac{3-e^2}{4(1-e)^3} + \gamma_1^2 + \gamma_2(e)\mathcal{G}(e).
\end{aligned}
\tag{14}
$$

The previous computations [Eqs. (13) and (14)] allow us to compute explicitly the following constants

$$\Upsilon_1 := \|\partial_e q\|_\infty \quad \text{and} \quad \Upsilon_2 := \left\|\partial_e^2 q\right\|_\infty .$$

Therefore,

$$|\Delta''(e)| \leq 2N\pi\mathcal{R}^2\Big(3\Upsilon_1 + \Upsilon_2\Big) := \mathcal{K}^*. \tag{15}$$

Appendix B: Initial conditions for the calculations

For completeness, we enclose the numerical values of the initial conditions for the vertical separation from the primaries plane. We take zero initial velocities to ensure the appropriate symmetry for the 15 branches analysed in this paper. They were computed by imposing periodic boundary conditions with fixed period equal to $T_N = 2N\pi$ and a closing condition of 10^{-12} for positions and velocities. These periodic orbits have been computed with a standard Dormand–Prince algorithm (Dormand and Prince 1980) and act as the initial solutions of the numerical continuation of the branches which have been performed with a tolerance of 10^{-10} in AUTO (Doedel et al. 1997) (Table 1).

Table 1 Initial vertical displacements for the 15 branches of symmetric periodic orbits analysed in this paper with a precision of 10^{-12}

p	$N = 1$	$N = 2$	$N = 3$
1	1.04379804265	1.84845961378	2.49539355255
2	0.44987027357	1.04379804265	1.47641674032
3	–	0.68497919388	1.04379804265
4	–	0.44987027357	0.78386153295
5	–	0.24569817368	0.59868635160
6	–	–	0.44987027357
7	–	–	0.31520742193
8	–	–	0.16550272001

Appendix C: Perturbative results

The initial orbits of the branches in this paper are solutions of the circular Sitnikov problem where the implicit Kepler equation is unnecessary. This solution along with the information of the linearized system allowed us following the technique of Galán et al. (2018) to derive explicit expression for many quantities at $e = 0$. Note that these results are completely independent of the continuation of the branches.

While trying to compare our branches with the computational results of Jiménez-Lara and Escalona-Buendía (2001), we found opposite signs for the initial slope of some of the branches. The authors of Jiménez-Lara and Escalona-Buendía (2001) make use of a highly nonlinear change of scales to separate the different families of curves that make difficult a direct comparison. To validate our continuation results, we have computed $\xi'(0)$ which is the slope of the branch at $e = 0$ in the bifurcation diagram.

An explicitly computable expression for the initial slope can be deduced in terms of the even, $2N\pi$-periodic solution $\varphi_p(t)$ of the circular Sitnikov problem that satisfies the initial value problem

$$\ddot{z} + \frac{z}{(z^2 + 1/4)^{3/2}} = 0, \quad z(0) = \xi_p, \quad \dot{z}(0) = 0.$$

From Theorem 1 and the equation (13) in Galán et al. (2018), the slope $\xi'(0)$ is given by

$$\xi'(0) = -\frac{\partial_e F_N(\xi_p, 0)}{\partial_\xi F_N(\xi_p, 0)},$$

where $F_N(\xi, e) = \dot{z}(N\pi, \xi(e), e)$, $e \in [0, e^*_{N,p}]$ and $\xi(e) := \mathcal{H}_{N,p}(e)$ with $\xi(0) = \xi_p$. Furthermore, a direct computation shows that the canonical solutions $y_1(t, e)$ and $y_2(t, e)$ of (5) for $e = 0$ satisfy

$$y_1(t, e) := \frac{\partial \varphi_p(t, \xi_p)}{\partial \xi}, \quad y_2(t, 0) := -\frac{\dot{\varphi}_p(t)}{f(\xi_p, 1/2)},$$

where $f(z, r) = \dfrac{z}{(z^2 + r^2)^{3/2}}$. Define

$$\phi_1(t) := y_1(t, 0) \quad \text{and} \quad \mu = f(\xi_p, 1/2).$$

Then

$$\phi_1(N\pi) = \frac{\partial \dot{\varphi}_p(t, \xi_p)}{\partial \xi} \quad \text{and} \quad \dot{y}_2(N\pi, 0) = -\frac{\ddot{\varphi}_p(N\pi)}{\mu} = -\frac{\varphi_p(N\pi)}{\mu f(\varphi_p(N\pi), 1/2)}$$

From here and the Eq. (28) in Galán et al. (2018), we have

$$\begin{aligned}
\partial_\xi F_N(\xi_p, 0) &= \dot{\phi}(N\pi), \\
\partial_e F_N(\xi_p, 0) &= -\frac{3}{4} \int_0^{N\pi} G_t(N\pi, s, 0) \frac{\varphi_p(s)\cos(s)}{\left(\varphi_p(s)^2 + \frac{1}{4}\right)^{\frac{5}{2}}} \, \mathrm{d}s,
\end{aligned}$$

where $G_t(t, s, e) = y_1(s, e)\dot{y}_2(t, e) - \dot{y}_1(t, e)y_2(s, e)$. Notice that

$$\begin{aligned}
\frac{G_t(N\pi, s, 0)}{\dot{y}_1(N\pi, 0)} &= \frac{y_1(s, 0)\dot{y}_2(N\pi, 0)}{\dot{y}_1(N\pi, 0)} - y_2(s, 0) \\
&= \frac{\dot{\varphi}_p(s)}{\mu} - \phi_1(s)\frac{\ddot{\varphi}_p(N\pi)}{\mu\,\dot{\phi}_1(N\pi)}.
\end{aligned}$$

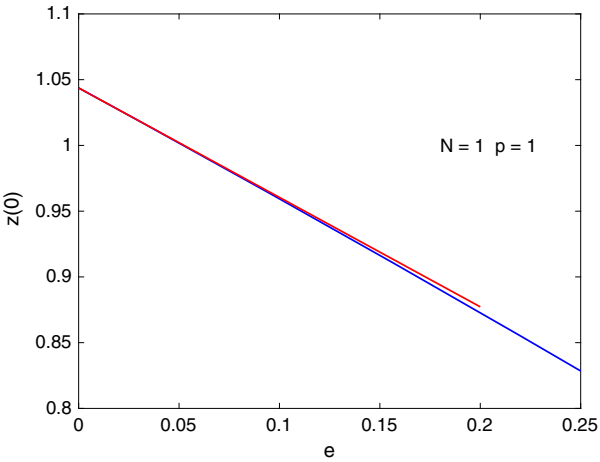

Fig. 10 Comparison of the computed branch (blue) and the linear approximation (red) with the slope computed by evaluating the slope with Eq. 16. In the ξ, e plot the branches emanates form the circular case with a negative slope and the linear approximation remains accurate up to $e \sim 0.2$

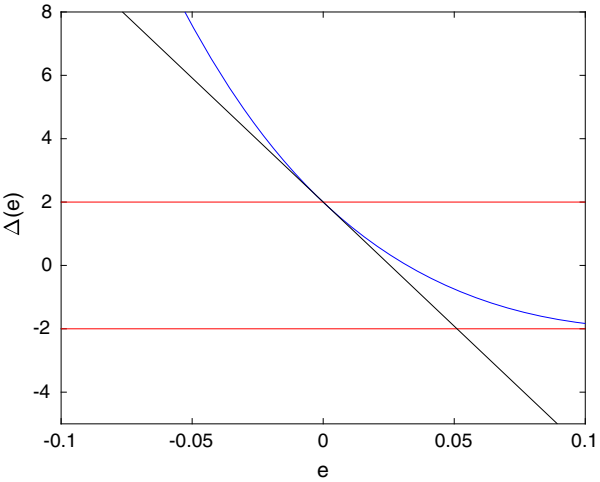

Fig. 11 Comparison of the computed behaviour of the discriminant function (blue) and the linear approximation (black) with the slope computed by evaluating the slope with Eq. 17 for $N = 2$ and $p = 1$. The red horizontal lines delimit the stable region

Finally, the explicit formula for the slope $\xi'(0)$ is given by

$$\xi'(0) = \frac{3}{4\mu} \int_0^{N\pi} \left(\dot{\varphi}_p(s) - \phi_1(s) \frac{\ddot{\varphi}_p(N\pi)}{\dot{\phi}_1(N\pi)} \right) \frac{\varphi_p(s)\cos(s)}{\left(\varphi_p(s)^2 + \frac{1}{4}\right)^{\frac{5}{2}}} \mathrm{d}s. \tag{16}$$

For the case $N = 1$ and $p = 1$, we have computed this initial slope for the 15 branches with excellent agreement. In Fig. 10, we plot the original branch (blue) and its linear approximation (red) for $e \in [0,\ 0.25]$.

The slope of the discriminant functions can be explicitly computed by a lengthy but straightforward calculation as shown in Section 4 of Galán et al. (2018). An even simpler but equivalent expression for $\Delta'(0)$ has been obtained in Zhang et al. (2018) in terms of the flow of the circular Sitnikov problem and the canonical solutions of its linearized version:

$$\Delta'(0) = \frac{\phi_1'(2N\pi, 0)}{4\mu^2} \int_0^{2N\pi} \frac{\cos s}{\left(\varphi(s)^2 + \frac{1}{4}\right)^{\frac{3}{2}}} \mathrm{d}s. \tag{17}$$

The numerical evaluation of this integral confirms the claim that for even values of N the discriminant function does not necessarily vanish. In the case of $N = 2$ and $p = 1$, the numerical value given by Eq. 17 is $\Delta'(0) = -78.34$ which matches perfectly the computed behaviour of the continuation calculation as shown in Fig. 11.

References

Belbruno, E., Llibre, J., Ollé, M.: On the families of periodic orbits which bifurcate from the circular Sitnikov motions. Celest. Mech. Dyn. Astron. **60**, 99–129 (1994)

Corbera, M., Llibre, J.: Periodic orbits of the Sitnikov problem via a Poincaré map. Celest. Mech. Dyn. Astron. **77**, 273–303 (2000)

Corbera, M., Llibre, J.: On symmetric periodic orbits of the elliptic Sitnikov problem via the analytic continuation method. In: Chenciner, A., Cushman, R., Robinson, C., Jeff Xia, Z. (eds.) Celestial Mechanics. Contemporary Mathematics, vol. 292, pp. 91–127. AMS, Providence (2002)

Doedel, E.J., Champneys, A.R., Fairgrieve, T.F., Kuznetsov, Y.A., Sandstede, B., Wang, X.J.: AUTO97: Continuation and Bifurcation Software for Ordinary Differential Equations (1997). http://indy.cs.concordia.ca

Dvorak, R.: Numerical results to the Sitnikov problem. Celest. Mech. Dyn. Astron. **87**, 71–80 (1993)

Dormand, J.R., Prince, P.J.: A family of embedded Runge–Kutta formulae. J. Comput. Appl. Math. **6**, 19–26 (1980)

Galán, J., Núñez, D., Rivera, A.: Quantitative stability of certain families of periodic solutions in the Sitnikov problem. SIAM J. App. Dyn. Syst. **17**, 52–77 (2018)

Galán-Vioque, J., Muñoz-Almaraz, F.J., Freire, E., Freire, E.: Continuation of periodic orbits in symmetric hamiltonian and conservative sytems. Eur. Phys. J. Top. **223**(13), 2705–2722 (2014)

Jury, E.I.: Inners and Stability of Dynamic Systems. Wiley, Hoboken (1975)

Jiménez-Lara, L., Escalona-Buendía, A.: Symmetries and bifurcations in the Sitnikov problem. Celest. Mech. Dyn. Astron. **79**, 97–117 (2001)

Libre, J., Simó, C.: Estudio cualitativo del problema de Sitnikov. Publicacions Mathemàtiques U.A.B **18**, 49–71 (1980)

Llibre, J., Ortega, R.: On the families of periodic orbits of the Sitnikov problem. SIAM J. Appl. Dyn. Syst. **7**, 561–576 (2008)

MacMillian, W.D.: An integrable case in the restricted problem of three bodies. Astron. J. **27**, 11–13 (1913)

Magnus, W., Winkler, S.: Hill's Equation. Dover, New York (1979)

Martínez-Alfaro, J., Chiralt, C.: Invariant rotational curves in Sitnikov's problem. Celest. Mech. Dyn. Astron. **55**, 351–367 (1993)

Muñoz-Almaraz, F.J., Freire, E., Galán-Vioque, J., Vanderbauwhede, A.: Continuation of normal doubly symmetric orbits in conservative reversible systems. Celest. Mech. Dyn. Astron. **97**(1), 17–47 (2007)

Muñoz-Almaraz, F.J., Freire, E., Galán-Vioque, J., Doedel, E.J., Vanderbauwhede, A.: Continuation of periodic orbits in conservative Hamiltonian systems. Physica D **181**, 1–38 (2003)

Ortega, R., Rivera, A.: Global bifurcations from the center of mass in the Sitnikov problem. Discrete Contin. Dyn. Syst. Ser. B **14**, 719–732 (2010)

Ortega, R.: The twist coefficient of periodic solutions of a time-dependent Newton's equation. J. Dyn. Differ. Equ. **4**, 651–665 (1992)

Ortega, R.: Periodic solutions of a newtonian equation: stability by the third approximation. J. Differ. Equ. **128**, 491–518 (1996)

Pavanini, G.: Sopra una nuova categoria di soluzioni periodiche nel problema di tre corpi. Annali di Mathematica, Serie III, Tomo XIII, pp. 179–202 (1907)

Perdios, E., Markellos, V.V.: Stability and bifurcations of Sitnikov motions. Celest. Mech. Dyn. Astron. **42**, 187–200 (1988)

Rivera, A.: Bifurcación de soluciones periódicas en el problema de Sitnikov. Ph.D. Thesis, Universidad de Granada (2012)

Robinson, C.: Uniform sub-harmonic orbit for Sitinikov problem. Discrete Contin. Dyn. Syst. Ser. S **1**, 647–652 (2008)

Sidorenko, V.: On the circular Sitnikov problem: the alternation of stability and instability in the family of vertical motions. Celest. Mech. Dyn. Astron. **109**, 367–384 (2011)

Soulis, P., Bountis, T., Dvorak, R.: Stability of motion in the Sitnikov 3-body problem. Celest. Mech. Dyn. Astron. **99**, 129–148 (2007)

Sitnikov, K.A.: Existence of oscillating motion for the three-body problem. Dokl. Akad. Nauk **133**, 303–306 (1960)

Tkhai, V.N.: Periodic motions of a reversible second-order mechanical system. Application to the Sitnikov problem. J. Appl. Math. Mech. **70**, 734–753 (2006)

Zhang, M., Cen, X., Cheng, X.: Linearized stability and instability of nonconstant periodic solutions of Lagrangian equations. Math. Methods Appl. Sci. **41**, 4853–4866 (2018)